

Drought impact on forest carbon dynamics and fluxes in Amazonia

Christopher E. Doughty^{1*}, D. B. Metcalfe², C. A. J. Girardin¹, F. F. Amezquita³, D. Galiano³, W. Huaraca Huasco³, J. E. Silva-Espejo³, A. Araujo-Murakami⁴, M. C. da Costa⁵, W. Rocha⁶, T.R. Feldpausch⁷, A. L. M. Mendoza³, A. C. L. da Costa⁵, P. Meir^{8,9}, O. L. Phillips¹⁰, Y. Malhi¹

¹*Environmental Change Institute, School of Geography and the Environment, University of Oxford, Oxford, U.K.*; ²*Department of Physical Geography and Ecosystem Science, Lund University Lund, Sweden*; ³*Universidad Nacional San Antonio Abad del Cusco, Cusco, Perú*; ⁴*Museo de Historia Natural Noel Kempff Mercado, Universidad Autónoma Gabriel René Moreno, Santa Cruz, Bolivia*; ⁵*Universidade Federal do Pará, Belém, Pará, Brazil*; ⁶*Amazon Environmental Research Institute (IPAM), Canarana, Mato Grosso, Brazil*; ⁷*Geography, College of Life and Environmental Sciences, University of Exeter, Exeter, U.K.*; ⁸*School of Geosciences, University of Edinburgh, UK*; ⁹*Research School of Biology, Australian National University, Canberra, Australia*; ¹⁰*School of Geography, University of Leeds, U.K.*

*Corresponding author: chris.doughty@ouce.ox.ac.uk

Running title – Impact of drought on Amazonia

Key words: Drought, Amazon, GPP, NPP, tropical forests, allocation

27 **Abstract** – In 2005 and 2010, the Amazon basin experienced two strong droughts¹, driven by shifts in
28 the tropical hydrological regime² possibly associated with global climate change³ as predicted by
29 some global models³. Tree mortality increased following the 2005 drought⁴ and regional atmospheric
30 inversion modelling showed basin-wide decreases in CO₂ uptake in 2010 compared to 2011⁵. But the
31 response of tropical forest carbon cycling to these droughts is not fully understood and there has not
32 been a detailed multi-site investigation *in situ*. Here we use several years of data from a network of 13
33 one hectare forest plots spread throughout South America, where each component of net primary
34 production (NPP), autotrophic (R_a) and heterotrophic respiration (R_h) is measured separately, to
35 develop a better mechanistic understanding of the impact of the 2010 drought on the Amazon forest.
36 We find surprisingly that total NPP remained constant throughout the drought. However, towards the
37 end of the drought, autotrophic respiration, especially in roots and stems, declined significantly
38 compared to measurements in 2009 made in the absence of drought, with extended decreases in
39 autotrophic respiration in the three driest plots. In the year following the drought, total NPP continued
40 to remain constant but the allocation of carbon shifts towards canopy NPP and away from fine root
41 NPP. Both leaf-level and plot-level measurements indicate that drought suppresses photosynthesis.
42 Scaling these measurements to the entire Amazon basin using rainfall data, we estimate that drought
43 suppressed Amazon-wide photosynthesis in 2010 by 0.38 Pg C (0.23 - 0.53 Pg C). Overall, we find
44 that during episodic drought, instead of reducing total NPP trees prioritized growth by reducing
45 autotrophic respiration. This suggests that trees reduce investment in tissue maintenance and defence,
46 in line with eco-evolutionary theories which hypothesize that trees are competitively disadvantaged in
47 the absence of growth⁶. We propose that weakened maintenance and defence investment may, in turn,
48 cause the increase in tree mortality following drought observed at our plots.

49

50

51

52 How does drought affect tropical forests? This question has been studied in long-term
53 experimental drought studies^{7,8}, long-term biomass plots that have tracked forest dynamics through
54 drought events⁴, and through remote sensing⁹⁻¹¹. Increased mortality of trees using a large network
55 of 1 ha plot censuses was observed following the 2005 Amazonian drought, turning the forest from an
56 estimated net biomass carbon (C) sink of $\approx 0.71 \text{ Mg C ha}^{-1} \text{ yr}^{-1}$ ¹² to a temporary net source of CO₂ to
57 the atmosphere of twice this, with a total impact (i.e., committed source minus baseline sink) of 1.2-
58 1.6 Pg C⁴. This increase in drought-induced tree mortality has also been seen in two multi-year
59 experimentally droughted plots in Amazonia, dominated by a sustained increase in large tree
60 mortality⁷. Remote sensing of canopy backscatter following the 2005 drought indicated that, in some
61 parts of Amazonia, the drought caused a change in structure and water content associated with the
62 forest upper canopy. This suggests a slow recovery (>4 y) of forest canopy structure after the severe
63 drought in 2005¹⁰.

64 Since future droughts in tropical regions may increase in frequency and severity¹⁻³, a better
65 understanding of whether net CO₂ fluxes to the atmosphere from tropical forests increase or decrease
66 during drought periods is urgently required. Drought could either suppress gross primary productivity
67 (GPP), which would lead to an immediate reduction of CO₂ uptake, or it could reduce heterotrophic
68 respiration thereby reducing the CO₂ source to the atmosphere, or both¹³. The Amazon basin in 2010
69 was drier than in 2011, but not warmer, enabling the separation of the influences of temperature and
70 precipitation⁵. A recent atmospheric inversion study in the Amazon basin found that forests took up
71 $0.25 \pm 0.14 \text{ Pg C less CO}_2$ in 2010 (the year of the drought) than 2011 after accounting for the effect of
72 increased fires during the drought⁵. A previous study using isotopic techniques found a similar result,
73 with the basin turning from a potential sink to a source following the dry El Niño year of 1997¹⁴.
74 These results indicate that annual Amazon droughts apparently suppress photosynthesis more than
75 respiration, but such a relative decrease has not been directly verified with on the ground
76 measurements.

77 To be able to understand long term carbon storage in the tropics, top-down estimates of GPP
78 and net respiration CO₂ fluxes to the atmosphere alone are insufficient. It is also important to
79 understand how the products of photosynthesis are allocated between plant metabolism and biomass
80 growth (net primary productivity, NPP) and how that growth is allocated amongst different organs of
81 the tree¹⁵. Total autotrophic respiration plus total NPP should approximately equal total GPP over
82 long (multi-year) timescales. However, over shorter timescales the two may differ as forests may
83 store 'old' carbon in the form of non-structural carbohydrates (NSC), which may be abundant in
84 tropical forests ($\sim 16 \text{ Mg C ha}^{-1}$, more than enough carbon to rebuild the entire leaf canopy)¹⁶. These

85 NSCs may function as a reserve that enables continuation of high rates of growth during periods of
86 reduced carbon income from photosynthesis¹⁶⁻¹⁸.

87 For several years, we have measured the main components of total NPP (including one to
88 three month records of fine root, woody, and leaf flush NPP) and autotrophic respiration (including
89 rhizosphere, stem wood, and canopy leaf respiration) at 13 one-hectare rainforest plots in three South
90 American countries, covering contrasting climatic and soil conditions and also across a 2800m
91 elevation range in the Andes (ED tables 1-3). Initial results from these measurements have been
92 described in a series of companion papers¹⁹⁻²³ presenting complete mean annual sums and mean
93 seasonal cycles of NPP and autotrophic respiration (R_a). This methodology has shown close
94 agreement with independent eddy covariance data on seasonal and annual timescales (ED Figure 1 –
95 slope is within the error of a one-to-one line - $3.0 \pm 7.8\%$ (95% confidence interval))²⁴. Here, we
96 synthesize and further analyse these results to focus specifically on the basin-wide trends before,
97 during and after the 2010 drought, constrained by concurrent measurements in a larger network
98 measuring woody NPP and mortality⁴ and inversion studies monitoring changes in atmospheric CO_2
99 concentrations⁵. Of the 13 plots, six experienced drought in 2010 (ED Figure 2). Of these six, three
100 can be considered lowland humid forest more typical of Amazonia (based on species composition and
101 maximum cumulative water deficit (MCWD)) and three are drier forests at the Amazon forests'
102 southern margins.

103 Throughout the two year period of study, the eight non-drought plots showed steady NPP, R_a ,
104 and total plant carbon expenditure (PCE - the sum of NPP and R_a or the carbon expended by the
105 autotrophic metabolism of the ecosystem; green line Figure 1). Total NPP was surprisingly invariant
106 throughout the drought period at all of our plots (Figure 1c). Among the six drought-affected plots,
107 there were differences between those in the dry lowlands (red lines, N=3) and those in the more
108 humid areas (black lines, N=3). PCE in the humid lowland plots was constant at the start of the
109 drought, but then both PCE and R_a decreased significantly ($P < 0.05$ and $P < 0.01$ respectively, paired T-
110 test, N=3 plots) through early 2011 relative to the 2009 baseline. The humid plots recovered to the
111 2009 baseline within a few months after the drought but decreases in R_a at the three dry lowland plots
112 persisted for a year after the 2010 drought (Figure 1b). This short-term decrease in R_a (dominated by
113 changes in rhizosphere and stem respiration - ED figure 7) is in contrast to the results from multi-
114 annual experimental drought where R_a increased (dominated by changes in leaf respiration)¹⁹.

115 PCE should approximately equal total photosynthesis in an ecosystem over annual to multi-
116 annual time scales, with any discrepancy between the two on shorter (monthly) timescales caused by
117 changes in unmeasured carbon pools such as non-structural carbohydrate reserves. Therefore, a
118 decrease in PCE must equal an equivalent decrease in GPP during a prior period. At our humid
119 drought sites, PCE decreased by $1.90 \pm 1.04 \text{ Mg C ha}^{-1} \text{ yr}^{-1}$ (95% C.I.) following the drought period
120 compared to the 2009 baseline (yellow region of Figure 1a). *In situ* measurements of light saturated

121 maximum photosynthesis made at a subset of our plots indicate that photosynthesis did decrease
122 significantly ($P < 0.001$, T-test, $N = 20$ trees) during the drought period compared to non-drought
123 conditions, pointing to the drought as the cause of the drop in PCE (ED Figure 3). This measured
124 decrease in photosynthesis is of a similar magnitude to modelled decreases in photosynthesis from
125 drought in Eastern Amazonia²⁵. We hypothesize that the asynchrony between the decrease in PCE
126 and the start of the drought indicates that the forests relied on non-structural carbohydrate reserves to
127 initially maintain constant growth and respiration during the drought period (ED Figure 4). Towards
128 the middle of the drought period, R_a decreased in the rhizosphere and stems, while NPP and growth
129 continued to remain relatively constant. Since autotrophic respiration consists of maintenance (non-
130 growth) respiration and the respiratory costs associated with growth, this suggests that maintenance
131 respiration must have declined. The decrease in R_a continued following the end of the drought period,
132 potentially allowing the replenishment of the NSC stores once normal photosynthesis resumed (ED
133 Figure 4). Drought reduced PCE by a larger amount in dry zone plots than in humid zone plots, with
134 total PCE continuing to decline through 2011. The greater total decline in PCE is indicative of a
135 larger percentage decrease in total photosynthesis during the drought at the drier plots, a plot-scale
136 observation which matches our *in situ*, leaf level measurements (ED Figure 3). Our data show little
137 change to net heterotrophic respiration in the humid plots (supplementary results and Figure 1d black
138 line), and this suggests that the drought forest plots were first a net C source in 2010 due to
139 suppressed photosynthesis, and then a net C sink in early 2011 as photosynthesis returned to normal,
140 whilst R_a in the stems and rhizosphere remained slightly suppressed compared to previous periods
141 (ED Figure 4 and 7).

142 There was strong seasonality in the components of NPP, with peaks in leaf growth
143 generally anti-correlated with the peaks in woody growth. Hence variation in seasonal growth rates
144 was driven more by shifts in allocation of NPP than by variation in its total magnitude²⁶. NPP
145 allocation in the non-droughted plots did not change significantly between 2009 and 2010 (Figure 2
146 green). In the droughted plots there were no significant shifts in allocation patterns during the drought
147 period itself, but in the 6 months following the drought there was a significant shift in C allocation for
148 both the humid and dry lowland plots following the drought period away from fine root growth
149 ($P < 0.01$, paired T-test, $N = 3$) and towards canopy growth (a combination of LAI and litterfall – see
150 methods - $P < 0.05$, paired T-test, $N = 3$) (Figure 2 red and black). Droughts typically increase leaf fall,
151 a strategy thought to minimize drought-induced xylem embolisms, and can cause temperature-related
152 leaf damage as evaporative cooling decreases⁸. Therefore, preferential allocation of carbon towards
153 the canopy in the year following the drought is consistent with known physiological drought
154 responses, and likely represents additional carbon required to replenish lost and damaged leaves and
155 thereby rebuild photosynthetic capacity. The significant shift away from fine root growth was
156 surprising since it has often been assumed that fine root growth might increase during a drought, but
157 may simply be a reflection of the immediate priority of replacing lost canopy cover instead of a long

158 term shift away from root growth (for longer-term allocation patterns see ED Figure 5 and a
159 companion paper²⁶).

160 Individual tree mortality rates approximately doubled at our droughted plots, showing a
161 marginally significant increase ($P=0.06$; paired 1-tailed T-test, $N=5$) from a long term mean of
162 $1.6\pm 0.6\%$ (Tambopata, $N=3$) and $2.0 \pm 0.4\%$ (Kenia, $N=2$) to peaks of 3.6% (Tambopata) and 6.7%
163 (Kenia) following the drought (ED figure 6). Mortality remained relatively stable at the non-drought
164 plots. We tested mortality in a bigger subset of plots at Tambopata and Caxiuanã going back ~30
165 years at some plots (supplementary results) and found that biomass loss rates increased significantly
166 ($P<0.05$, Wilcoxon signed rank test) at Tambopata (drought, $N=9$) but not at Caxiuanã (no drought,
167 $N=6$). Committed carbon released due to mortality increased by ~1 and 3 fold in Kenia and
168 Tambopata respectively, compared to a $1.6\% \text{ yr}^{-1}$ basin wide average (Figure 3e)²⁷. Similar drought-
169 induced mortality was also seen across the wider basin following the 2005 drought⁴. The Bolivian
170 plots experienced more severe drought ($\text{MCWD}_{\text{anom}} < -240 \text{ mm}$) and here, more trees died more
171 quickly than in the Peruvian plots which were less strongly droughted ($\text{MCWD}_{\text{anom}} = -51 \text{ mm}$). Our
172 data indicate that mortality rates peaked 1-2 years after the drought, consistent with the hypothesis
173 that trees were weakened during the drought from reduced maintenance but only succumbed later¹⁹.

174 Plant carbon expenditure was significantly related ($P<0.05$, linear regression) and
175 autotrophic respiration was marginally significantly related ($P=0.08$, linear regression) to the anomaly
176 in MCWD for both annual sums ($N=13$ individual plots for 2009 minus 2010, $\text{PCE}_{\text{anom}} = -1.0 + 0.011 * \text{MCWD}_{\text{anom}}$,
177 $r^2 = 0.34$, with a standard error on the slope of ± 0.004 , Figure 3a and b). The anomaly in
178 NPP, on the other hand, showed no significant relationship with the MCWD anomaly (Figure 3c,
179 $P>0.10$). We combine a TRMM (v7 years 1998-2012) based $\text{MCWD}_{\text{anom}}$ for each TRMM pixel in the
180 Amazon in 2010 and 2011 with the slope of the above equation (with an intercept of zero) to estimate
181 that mean net total photosynthesis decreased by 0.38 Pg C (0.23 - 0.53 Pg C) in 2010 compared to
182 2011, based on a mean South American tropical forested area of $6.77 \times 10^6 \text{ km}^2$ (Figure 3d). For the
183 same period, an Amazonia-focussed atmospheric inversion modelling study estimated a decreased
184 flux of $0.25 \pm 0.14 \text{ Pg C}$ in 2010 relative to 2011 from reduced photosynthesis, which is within our
185 error estimates⁵.

186 Why would trees prioritize growth over maintenance or defence during and following a
187 drought? This strategy makes sense when viewed from an eco-evolutionary standpoint where any
188 decrease in growth of an individual tree puts that tree at a competitive disadvantage by increased risk
189 of loss of resources (light, water, or nutrients) to neighbours⁶. We hypothesize that this decrease in
190 maintenance and defence led to our plot-level increase in mortality. Thus, while such a drought-
191 induced strategy may reduce the mean per-tree performance in the forest via increased mortality, it is
192 still likely to be selected for on an individual basis given the evolutionary constraints proposed by

193 game theory²⁸. In other words, this strategy increases mortality for a small proportion of trees
194 because most are locked in to growth competition with neighbours. Such unexpected carbon
195 allocation patterns have been theorized previously, but before now have lacked much empirical
196 support. For instance, trees may grow excess leaves not to improve carbon uptake but to shade out
197 competition²⁹ or they may over-allocate carbon to root growth in shallow soil systems in response to
198 competition⁶.

199 Overall, our plot data indicate that drought suppressed total CO₂ uptake with little
200 reduction in growth and therefore, less carbon was available to the trees for defence and maintenance.
201 Reduced carbon would have also increased tree mortality from embolisms and cavitation because
202 non-structural carbohydrates (sugars) may be involved in sensing and reversing embolism¹⁸. The
203 debate over drought-induced tree mortality is often framed as being caused by either C starvation,
204 water cavitation, or biotic attack, but the three are often intertwined³⁰ because during drought there is
205 less C available to fend off all three threats. This insight and new mechanistic understanding can help
206 to improve predictions of the impact of future climate change on tropical forests.

207

208

209

210 **Acknowledgements** - This work is a product of the Global Ecosystems Monitoring (GEM) network
211 (gem.tropicalforests.ox.ac.uk) and the RAINFOR and ABERG research consortia, and was funded by
212 grants to YM and OP from the Gordon and Betty Moore Foundation to the Amazon Forest Inventory
213 Network (RAINFOR) and the Andes Biodiversity and Ecosystems Research Group (ABERG), and
214 grants from the UK Natural Environment Research Council (Grants NE/D01025X/1, NE/D014174/1,
215 and NE/F002149/1, NE/J011002/1), the NERC AMAZONICA consortium grant (NE/F005776/1),
216 the EU FP7 Amazalert (282664) GEOCARBON (283080) projects. Some data in this publication
217 were provided by the Tropical Ecology Assessment and Monitoring (TEAM) Network, a
218 collaboration between Conservation International, the Missouri Botanical Garden, the Smithsonian
219 Institution, and the Wildlife Conservation Society, and partially funded by these institutions, the
220 Gordon and Betty Moore Foundation, and other donors. We thank P. Brando and Tanguero partners
221 for logistical support and advice. TRF is supported by a National Council for Scientific and
222 Technological Development (CNPq, Brazil) award. PM is supported by an ARC fellowship award
223 FT110100457; OLP is supported by an ERC Advanced Investigator Award and a Royal Society
224 Wolfson Research Merit Award; YM is supported by an ERC Advanced Investigator Award and by
225 the Jackson Foundation. CED acknowledges funding from the John Fell Fund.

226

227

228 **Author contributions** – CED, YM, and DBM designed and implemented the study. CED analysed
229 the data. CED, CAJG, FFA, DG, WHH, JES, AA, MCC, ACLC, TF, AM, WR, and OP collected the
230 data. CED wrote the paper with contributions from YM, OP, PM, and DBM.

231

232 **Summary statement** - Monthly averaged data for all our plots used to calculate the results are
233 available in the supplementary material. Detailed plot descriptions for each plot are available in a
234 series of companion papers (^{19-23,32-33}). All raw data inputs are available upon request from the
235 authors or from <http://gem.tropicalforests.ox.ac.uk/>.

237 **References**

- 238 1 Lewis, S. L., Brando, P. M., Phillips, O. L., van der Heijden, G. M. F. & Nepstad, D. The 2010
239 Amazon Drought. *Science* **331**, 554-554, doi:DOI 10.1126/science.1200807 (2011).
- 240 2 Gloor, M. *et al.* Intensification of the Amazon hydrological cycle over the last two decades,.
241 *Geophys. Res. Lett* **40**, doi:10.1002/grl.50377 (2013).
- 242 3 IPCC. Synthesis Report, Summary for Policymakers. *An Assessment of the Intergovernmental*
243 *Panel on Climate Change* (2007).
- 244 4 Phillips, O. L. *et al.* Drought Sensitivity of the Amazon Rainforest. *Science* **323**, 1344-1347,
245 doi:DOI 10.1126/science.1164033 (2009).
- 246 5 Gatti, L. V. *et al.* Drought sensitivity of Amazonian carbon balance revealed by atmospheric
247 measurements. *Nature* **506**, 76+, doi:Doi 10.1038/Nature12957 (2014).
- 248 6 Franklin, O. *et al.* Modeling carbon allocation in trees: a search for principles. *Tree Physiol*
249 **32**, 648-666, doi:DOI 10.1093/treephys/tpr138 (2012).
- 250 7 da Costa, A. C. L. *et al.* Effect of 7 yr of experimental drought on vegetation dynamics and
251 biomass storage of an eastern Amazonian rainforest. *New Phytol* **187**, 579-591, doi:DOI
252 10.1111/j.1469-8137.2010.03309.x (2010).
- 253 8 Nepstad, D. C. *et al.* The effects of partial throughfall exclusion on canopy processes,
254 aboveground production, and biogeochemistry of an Amazon forest. *J Geophys Res-Atmos*
255 **107**, doi:Artn 8085 Doi 10.1029/2001jd000360 (2002).
- 256 9 Xu, L. A. *et al.* Widespread decline in greenness of Amazonian vegetation due to the 2010
257 drought. *Geophys Res Lett* **38**, doi:Artn L07402 Doi 10.1029/2011gl046824 (2011).
- 258 10 Saatchi, S. *et al.* Persistent effects of a severe drought on Amazonian forest canopy. *P Natl*
259 *Acad Sci USA* **110**, 565-570, doi:DOI 10.1073/pnas.1204651110 (2013).
- 260 11 Saleska, S. R., Didan, K., Huete, A. R. & da Rocha, H. R. Amazon forests green-up during 2005
261 drought. *Science* **318**, 612-612, doi:DOI 10.1126/science.1146663 (2007).
- 262 12 Phillips, O. L. *et al.* Changes in the carbon balance of tropical forests: Evidence from long-
263 term plots. *Science* **282**, 439-442, doi:DOI 10.1126/science.282.5388.439 (1998).
- 264 13 Meir, P., Metcalfe, D. B., Costa, A. C. L. & Fisher, R. A. The fate of assimilated carbon during
265 drought: impacts on respiration in Amazon rainforests. *Philos T R Soc B* **363**, 1849-1855,
266 doi:DOI 10.1098/rstb.2007.0021 (2008).
- 267 14 Townsend, A. R., Asner, G. P., White, J. W. C. & Tans, P. P. Land use effects on atmospheric
268 C-13 imply a sizable terrestrial CO₂ sink in tropical latitudes. *Geophys Res Lett* **29**, doi:Artn
269 1426 Doi 10.1029/2001gl013454 (2002).
- 270 15 Malhi, Y., Doughty, C. & Galbraith, D. The allocation of ecosystem net primary productivity in
271 tropical forests. *Philos T R Soc B* **366**, 3225-3245, doi:DOI 10.1098/rstb.2011.0062 (2011).
- 272 16 Wurth, M. K. R., Pelaez-Riedl, S., Wright, S. J. & Korner, C. Non-structural carbohydrate pools
273 in a tropical forest. *Oecologia* **143**, 11-24, doi:DOI 10.1007/s00442-004-1773-2 (2005).
- 274 17 Dietze, M. C. *et al.* Nonstructural Carbon in Woody Plants. *Annu Rev Plant Biol* **65**, 667-687,
275 doi:DOI 10.1146/annurev-arplant-050213-040054 (2014).
- 276 18 Sala, A., Woodruff, D. R. & Meinzer, F. C. Carbon dynamics in trees: feast or famine? *Tree*
277 *Physiology* **32**, 764-775, doi:DOI 10.1093/treephys/tpr143 (2012).
- 278 19 da Costa, A. C. L. *et al.* Ecosystem respiration and net primary productivity after 8-10 years of
279 experimental through-fall reduction in an eastern Amazon forest. *Plant Ecol Divers* **7**, 7-24,
280 doi:Doi 10.1080/17550874.2013.798366 (2014).
- 281 20 Araujo-Murakami, A. *et al.* The productivity, allocation and cycling of carbon in forests at the
282 dry margin of the Amazon forest in Bolivia. *Plant Ecol Divers* **7**, 55-69, doi:Doi
283 10.1080/17550874.2013.798364 (2014).

- 284 21 Doughty, C. E. *et al.* The production, allocation and cycling of carbon in a forest on fertile
285 terra preta soil in eastern Amazonia compared with a forest on adjacent infertile soil. *Plant*
286 *Ecol Divers* **7**, 41-53, doi:Doi 10.1080/17550874.2013.798367 (2014).
- 287 22 Malhi, Y. *et al.* The productivity, metabolism and carbon cycle of two lowland tropical forest
288 plots in south-western Amazonia, Peru. *Plant Ecol Divers* **7**, 85-105, doi:Doi
289 10.1080/17550874.2013.820805 (2014).
- 290 23 Rocha, W. *et al.* Ecosystem productivity and carbon cycling in intact and annually burnt
291 forest at the dry southern limit of the Amazon rainforest (Mato Grosso, Brazil). *Plant Ecol*
292 *Divers* **7**, 25-40, doi:Doi 10.1080/17550874.2013.798368 (2014).
- 293 24 Fenn, K., Malhi, Y., Morecroft, M., Lloyd, C. & Thomas, M. The carbon cycle of a maritime
294 ancient temperate broadleaved woodland at seasonal and annual scales. *Ecosystems* (in
295 press).
- 296 25 Fisher, R. A. *et al.* The response of an Eastern Amazonian rain forest to drought stress:
297 results and modelling analyses from a throughfall exclusion experiment. *Global Change Biol*
298 **13**, 2361-2378, doi:DOI 10.1111/j.1365-2486.2007.01417.x (2007).
- 299 26 Doughty, C. E. *et al.* Allocation trade-offs dominate the response of tropical forest growth to
300 seasonal and interannual drought. *Ecology* **95**, 2192-2201 (2014).
- 301 27 Lewis, S. L. *et al.* Concerted changes in tropical forest structure and dynamics: evidence from
302 50 South American long-term plots. *Philos T Roy Soc B* **359**, 421-436, doi:DOI
303 10.1098/rstb.2003.1431 (2004).
- 304 28 King, D. A. A Model Analysis of the Influence of Root and Foliage Allocation on Forest
305 Production and Competition between Trees. *Tree Physiol* **12**, 119-135 (1993).
- 306 29 Hikosaka, K. & Anten, N. P. R. An evolutionary game of leaf dynamics and its consequences
307 for canopy structure. *Funct Ecol* **26**, 1024-1032, doi:DOI 10.1111/j.1365-2435.2012.02042.x
308 (2012).
- 309 30 McDowell, N. G. *et al.* The interdependence of mechanisms underlying climate-driven
310 vegetation mortality. *Trends Ecol Evol* **26**, 523-532, doi:DOI 10.1016/j.tree.2011.06.003
311 (2011).

312

313

314

315 **Figure legends**

316 **Figure 1 –Impact of drought on carbon fluxes.** (a) Total plant carbon expenditure (PCE), (b) total
317 autotrophic respiration (R_a), (c) total net primary production (NPP), and (d) heterotrophic soil
318 respiration (R_h) by the forests for the three drought-affected forest plots in humid lowland zones (solid
319 black), in dry lowland zones (solid red), and the eight non-drought plots (solid green). Error bars
320 indicate the standard error of mean plot differences. For visual clarity we do not include all error
321 bars. Dashed lines show “normal” (2009; pre-drought) estimates smoothed with a span of 5 months
322 during 2010 and 2011 for the lowland plots (black dashed) and the dry lowland plots (red dashed).
323 The vertical bar labelled “drought” represents the approximate period of the drought. The areas
324 highlighted in yellow represents the drought anomaly or the impact of the drought on total plant
325 carbon expenditure (numerically equivalent to GPP) and R_a .

326

327 **Figure 2 –Impact of drought on carbon allocation.** (a) Total NPP, (b) mean carbon allocation to
328 canopy, (c) to wood, (d) to fine roots for non-drought lowland plots (green solid line; N=8), drought
329 plots in the humid lowlands (black solid lines; N=3), and drought plots in the dry lowlands (red
330 dashed lines; N=3). On the right (e-h) are the seasonally detrended anomaly data for each variable on
331 the left. All error bars are standard errors across plots. The vertical bar labelled “drought” represents
332 the approximate period of the drought. Significant change is determined with paired t-test comparing
333 six month periods during and following the drought to equivalent months in 2009 for all plots.

334

335 **Figure 3 – Estimated impact of drought on the basin-wide flux of CO_2** - The shifts in annual
336 fluxes in 2010 relative to 2009 for each individual plot for (a) plant carbon expenditure (PCE; equal to
337 GPP over longer time scales), (b) autotrophic respiration (R_a) and (c) total Net Primary Production
338 (NPP), plotted against the shift in maximum cumulative water deficit (MCWD) in 2010 relative to
339 2009. (d) Estimate of basin-wide anomaly in Gross Primary Production (2011 minus 2010; assumed
340 equal to PCE) based on the TRMM v7 calculated CWD anomaly ($mm\ month^{-1}$) and the slope of the
341 linear regression found in Figure 3a. We contrast 2010 to 2011 to compare with the atmospheric
342 inversion measurements collected during this period⁵. (e) Mortality rates as fraction of plot biomass
343 for Peruvian drought plots (grey line, N=3, error bars are s.e.), Bolivian drought plots (black line,
344 N=2), and no drought plots (red line, N=3). Mean Amazonian background tree mortality (no drought)
345 is shown as a black horizontal dashed line (from Lewis et al. 2004 Figure 3)²⁷.

346

347 **Methods** – We measured total NPP and autotrophic respiration at 13 one ha plots (plots described
348 individually below) throughout the Amazon basin through 2009-2010 (and 2009-2011 or 2009-2012
349 for droughted plots). A detailed description of each measurement is listed in ED Tables 1-3. Total
350 measured NPP included canopy, woody, and fine root NPP. In our seasonal estimates of NPP we
351 exclude several smaller components such as branchfall (although these data are shown in ED figure 6
352 and described in ED Tables 1-3), herbivory, coarse root, and small tree NPP (<10cm) that we have
353 included in previous estimates of these sites. We calculate leaf flush by calculating the change in leaf
354 area index, LAI ($\text{m}^2 \text{m}^{-2}$), multiplied by the mean specific leaf area, SLA ($\text{m}^2 \text{g}^{-1}$), and adding this to
355 leaf litterfall following a procedure from Doughty and Goulden (2008)³¹. Total estimated autotrophic
356 respiration consisted of rhizosphere respiration (i.e. respiration from roots, mycorrhizae and exudate-
357 dependent soil microbes), woody respiration and canopy respiration. Each component was measured
358 every 1-3 months, except for canopy respiration, which was measured only 1-2 times per plot at the
359 leaf level but scaled to the canopy scale using monthly LAI partitioned in sun and shade components.
360 Seasonal changes in autotrophic respiration during and following drought are due to monthly
361 measured rhizosphere and woody respiration, not canopy respiration (ED Figure 7). Detailed
362 information on the methodology and graphs showing data from each individual component are also
363 available from a series of companion papers^{19-23,32-33}. Each of these site papers includes a full spatial
364 and scaling error analysis for each measurement so we do not include them here for brevity.

365 *Photosynthesis* - Leaf photosynthesis was measured in Bolivia in the peak of the drought (Nov 2010)
366 and during a non-drought period (June 2011) on the same ~20 individual trees (12 different species
367 from plot A and 17 species from plot B) in the plot using canopy top cut branches (immediately recut
368 under water to restore hydraulic conductivity). These measurements are compared with leaf
369 photosynthesis measurements in the Tapajos, Brazil on attached (not cut) canopy top leaves accessed
370 via three walk up towers, to show that A_{sat} (light saturated photosynthesis) would not necessarily be
371 expected to decrease during a typical dry season and the measurements were taken at the start of a
372 typical dry season to near the end (ED Figure 3- methodological details in ED Tables 1-3).

373 *Climate* - We classified our drought sites according to cumulative water deficit (CWD) anomalies
374 based on precipitation data collected from automatic weather stations at each of the plots (AWS)
375 (Skye Instruments, Llandrindod, UK). Six of our 13 plots experienced drought in 2010 (negative
376 CWD anomalies more than half the year) with a mean CWD anomaly of -107 mm in October and a
377 mean MCWD of -135 mm, meaning that the driest month on average had a water deficit 135 mm
378 greater than a normal year (ED Figure 2). This varied regionally with the highest MCWD in the
379 Bolivian sites ($\text{MCWD}_{\text{anom}} = -240 \text{ mm}$) and the lowest in the lowland Peruvian sites ($\text{MCWD}_{\text{anom}} = -$
380 51 mm). We use Tropical Rainfall Monitoring Mission (TRMM) data from Jan 1998 to Dec 2012
381 (TRMM version 7) to calculate for each pixel the maximum monthly CWD anomaly (ED Figure 2).
382 The basin wide median $\text{MCWD}_{\text{anom}}$ for 2010 for droughted tropical forest regions was 136 mm
383 (excluding $\text{MCWD}_{\text{anom}} \geq 0 \text{ mm}$). This implies that the mean of our droughted plots had equivalent
384 moisture anomaly to the basin-wide “typical” Amazon drought for 2010 (ED Figure 2), but also that
385 our plots did not experience the more severe drought seen by some regions of Amazonia.

386
387 *Statistics* –All data were tested for normality and if they were normal, we did a two-tailed paired t-test
388 using Sigmaplot (Systat Software inc., San Jose, Ca, USA). If normality was not passed, as with the
389 mortality data, we used a Wilcoxon Signed Rank Test. We used a two-tailed test except for mortality
390 where we expect the change to be in one direction and therefore used a one-tailed test. We calculated
391 95% confidence intervals by multiplying the standard error by 1.96.

392
393 *Additional Mortality data* - For the additional RAINFOR analyses for Tambopata and Caxiuanã,
394 interval-by-interval loss rates in each plot were computed following standard RAINFOR field and
395 ForestPlots.net data protocols (see for example Quesada et al. 2012 and Lopez-Gonzalez et al.
396 2011)³⁴⁻³⁵. At Caxiuanã, data were collected by the TEAM network whose protocols are closely based
397 on RAINFOR models. These include multiple repeated diameter measurements of the same tree at
398 1.3m or above buttresses - allowing where necessary for point of measurement changes -, high-
399 resolution botanical identifications of hundreds of tree species at each site, and the use of taxon-

400 specific wood density values, to derive from each individual tree ≥ 10 cm diameter the stand-level
401 values of biomass and biomass dynamics. We used a generalized region-specific height-diameter
402 biomass allometry³⁶. Because here the question is simply whether the 2010 drought coincided with
403 mortality changes in each site, and not what the precise values of mortality were for individual
404 intervals and plots, we did not attempt to account for the small effects of slightly varying census-
405 interval lengths on wood production rates. Data were downloaded from ForestPlots.net in October
406 2014, and the TEAM database in April 2013.
407

408 *Site descriptions of 13, one ha plots*

409 *Plots with drought in 2010*

410 *Kenia (N=2, 1 ha plots)* - These plots were established and monitored on private property at
411 the Hacienda Kenia in Guarayos Province, Santa Cruz, Bolivia (16.0158° S, 62.7301° W) from
412 January 2009. The plots are 2 km apart, and are situated on inceptisols with relatively high fertility
413 (high cation exchange capacity and phosphorus concentration) and low acidity compared with eastern
414 Amazonian forests. The plots experienced almost identical climate and had sandy loam soil with 76%
415 sand content. However, one plot was located on a shallow soil (< 1 m depth) over pre-Cambrian
416 bedrock, leading to lower available water (we term this plot Kenia-B). The second plot was located on
417 deeper soils in a slight topographic depression (henceforth termed Kenia-A). These differences in
418 drainage and soil depth had an effect on forest composition at this ecotone, with Kenia-A hosting a
419 more humid forest type typical of Amazonian forests and Kenia-B a drier forest type typical of
420 *chiquitano* dry forests. For further details see Araujo-Murakami et al. 2014²⁰.

421 *Tanguro (N=2, 1 ha plots)* - The study area is located on the Fazenda Tanguro (~80,000 ha)
422 in Mato Grosso state, about 30 km north of southern boundary of the Amazon rainforest in Brazil
423 (13.0765° S, 52.3858° W). The soil type at the site is a red-yellow alic dystrophic latosol (RADAM
424 Brazil, 1974; Brazilian soil classification), a relatively infertile sandy ferralsol (FAO classification) or
425 oxisol (Haplustox; U.S. Department of Agriculture classification scheme), the groundwater is at about
426 15 m depth, and no layers of soil prevent root penetration through the soil profile. These soils are
427 amongst the least fertile in Amazonia and widespread across eastern Amazonia. The vegetation is
428 closed canopy, old growth forest with a relatively low mean canopy height (20 m) and relatively low
429 plant species diversity (97 species of trees and lianas greater than 10 cm DBH (diameter at 1.3 m stem
430 height above the ground)) when compared with the wetter forests typical of the central Amazon. For
431 further details see Rocha et al. 2014²³.

432 *Tambopata (N=2, 1 ha plots)* - The two study plots are located in the Tambopata reserve
433 (TAM-05 12.837° S, 69.2937° W and TAM-06 12.828° S, 69.2690° W), in the Madre de Dios region
434 of Peru. The geomorphology of the study region is based on old floodplains of the meandering
435 Tambopata River. TAM-05 is situated on a Pleistocene terrace (< 100,000 years old). The soil at
436 TAM-05 is a haplic cambisol (WRB taxonomy), and that at TAM-06 is a haplic alisol³⁷. We
437 incorporate mortality data from an additional nearby plot (TAM-09). No hardpan layers of soil
438 prevent root penetration through the soil profile. For further details see Malhi et al. 2014²².

439 We divide these six plots into three lowland plots (TAM-05, TAM-06, and Kenia-A - black
440 lines figure 1 and 2) and three dry-lowland plots (2 Tanguro plots and Kenia-B - red lines figure 1 and
441 2). Distinction of dry-lowland plots is made by using mean MCWD for Tanguro and by species
442 composition for Kenia-B with drier forest type species typical of *chiquitano* dry forests.
443

444 *Plots with no drought in 2010*

445 *San Pedro (N=2, 1 ha plots)* - The San Pedro site (13.0491°S, 71.5365°W) is located in
446 the Kosñipata Valley, in the cultural buffer zone of the Parque Nacional del Manú, Cusco, Peru. The
447 two plots at San Pedro lie very close to the transition between upper and pre-montane forest zones,
448 which occurs in this valley at approximately 1500-2000 m. Although data on cloud cover frequency
449 and cloud base elevation in the plots over the annual cycle are difficult to obtain, SP 1750 is immersed
450 for longer periods than SP 1500 during the austral winter months. SP 1500 is estimated to be near the
451 lower limit of the cloud base. For further details see Huasco et al. 2014³³.

452 Wayqecha ($N=2$, 1 ha plots) - The Wayqecha (RAINFOR plot code WAY-01: 13.1751°S
453 71.5948°W) and Esperanza (RAINFOR plot code ESP-01) plots are high elevation cloud forest
454 located in the cultural buffer zone of the Parque Nacional del Manú, Cusco, Peru at ~3000 meters
455 elevation. The two plots lie a few hundred metres below the treeline transition to high elevation
456 grasslands. For further details see Girardin et al. 2014³².

457 Caxiuanã-(CAX-08 and CAX-06) ($N=2$, 1 ha plots) – These plots are located in Caxiuanã
458 National Forest Reserve, Pará in the eastern Brazilian Amazon. Terra Preta (1.8560° S, 51.4352° W)-
459 The *terra preta* plot (plot code CAX-08 in the RAINFOR Amazon forest inventory network) was a
460 late successional forest with a large proportion of fruit trees, on an isolated patch (< 2 ha) of fertile
461 dark earth or *terra preta do Indio*. The original ferralsol soils became progressively enriched by the
462 activities of local inhabitants between the years of 1280 to 1600AD³⁸. The species composition of the
463 *terra preta* plot was that of an old abandoned agroforestry system, with Brazil nut (*Bertholletia*
464 *excelsa*), kapok (*Ceiba pentandra*) and also paleotropical tree crops including coffee (*Coffea*) and
465 orange (*Citrus*). The water-side location of the *terra preta* plot results in a substantially different
466 microclimate from that of the inland tower plot, with high solar radiation (the large cool water area of
467 the bay suppresses cloud formation close to the bay) and higher temperatures. The *tower* plot (CAX-
468 06) (1.7198 S, 51.4581 W) was a tall primary forest (35 m canopy height) situated on a clay-rich geric
469 alumnitic ferralsol (alumnitic, hyperdistric, clayic), near an eddy covariance flux tower, with species
470 composition typical of eastern Amazonia. For further details see Doughty et al. 2014²¹.

471 Caxiuanã-(TFE-control) – ($N=1$, 1 ha plots) This control plot of an experimental drought
472 study is approximately 2 km south of the tower plot mentioned above (1.7279°S, 51.468° W). It is a
473 largely undisturbed *terra firme* forest, of the type widespread across eastern Amazonia. The study plot
474 is located on highly weathered vetic acrisols typical of upland forests in the eastern Amazon, with a
475 thick stony laterite layer at 3–4 m depth. The site elevation is 15 m above river level in the dry season
476 and the water table has been occasionally observed at a soil depth of 10 m during the wet season. For
477 further details see da Costa et al. 2014¹⁹.

478 **Extended Data results –**

479 *Heterotrophic respiration* - Soil heterotrophic respiration showed no significant change during the
480 drought period in the droughted *humid* lowland plots (Figure 1d black line, $N=3$) and no significant
481 change with cumulative water deficit (CWD) anomaly ($P>0.05$). There was a slight suppression of
482 R_H near the start of the drought, but this was compensated by a larger than normal increase in R_H later
483 in the drought as some rains (although much lower than normal) arrived (Figure 1d black line).
484 However, in contrast, the droughted *dry* lowland plots did show a large decrease in soil heterotrophic
485 respiration at the start of the drought in comparison to 2009 (although only marginally significant
486 $P<0.1$, $N=3$) (Figure 1d red line), but these regions are a geographically small part of the basin and
487 their overall influence on basin wide fluxes is likely to be small. Mean temperatures were similar in
488 2010 and 2011 and therefore any change in heterotrophic flux was most likely to have been moisture
489 driven (ED Figure 2). Dead wood respiration was initially suppressed during the dry season of the
490 drought year but this was compensated by a large gain once the rains started, leading to no net annual
491 change in dead wood respiration from the drought (ED figure 6). Branch fall did not increase during
492 the drought and, in fact, slightly decreased, possibly because of lower wind speeds from reduced
493 storm activity (ED figure 6). Our data show little net change to heterotrophic respiration, and
494 therefore we estimate that the drought forest plots were first a net C source in 2010 due to suppressed
495 photosynthesis, and then a net C sink in early 2011 as photosynthesis returned to normal but R_a
496 remained slightly suppressed compared to previous periods, an observation which is in line with a
497 recent atmospheric inversion study of the Amazon basin⁵.

498
499 *Carbon Allocation shifts*- In two of the plots (Kenia A and B), NPP allocation shifted towards roots in
500 the second year after the drought, possibly to alleviate water stress for future droughts, or to increase
501 nutrient uptake to track recovered carbon uptake (ED Figure 5 – NPP allocation patterns at this site
502 are explored in detail in a companion paper²⁶). However, allocation responses to drought vary
503 strongly by site. For instance, in two lowland Peruvian plots that experienced milder drought, NPP

504 instead shifted back towards woody growth in the second year following the drought (ED Figure 5)
505 while in two dry lowland Brazilian plots that experienced moderate drought, woody growth increased
506 in the year following the drought at the expense of canopy and fine root growth (ED Figure 5). The
507 two plots hardest hit by the drought ($MCWD_{anom} = -240$ mm) showed a long term decrease in
508 allocation of NPP towards wood even though total NPP remained constant (ED Figure 5). This
509 indicates that care should be taken in the interpretation of tree growth and dendrochronology results as
510 proxies for productivity following drought as they may be more influenced by shifting carbon
511 allocation than by changes in total NPP. Our plots show no significant change in woody NPP growth
512 rates during the drought although there is a small decline (Figure 2). Woody growth rates may
513 actually decline, but our sample size of three is too small to capture the signal statistically.

514
515 *Additional mortality results-* To see if mortality increased more broadly in the regions surrounding
516 our plots, we compared plots in the RAINFOR database near Tambopata (with drought according to
517 our meteorological station data) to Caxiuanã (without drought in 2010). In Caxiuanã, we compared
518 plots 1 to 6 (= TEC-01 to TEC-06 using the RAINFOR code) for pre-2010 mortality (starting in 2003)
519 to mortality from a census in late 2010. In Tambopata, we compared plots TAM-01 to TAM-08 for
520 pre-2010 mortality (mostly starting in 1983) to mortality from a census in mid-2011. For this dataset,
521 we use a non-parametric Wilcoxon signed rank test and find significant increase in biomass mortality
522 following the 2010 drought in the larger Tambopata dataset ($N = 9$, $p = 0.018$). We contrast this to
523 Caxiuanã (a no drought site) where we also have high resolution met station data and find no
524 significant change following 2010 ($N=6$, $p>0.05$).

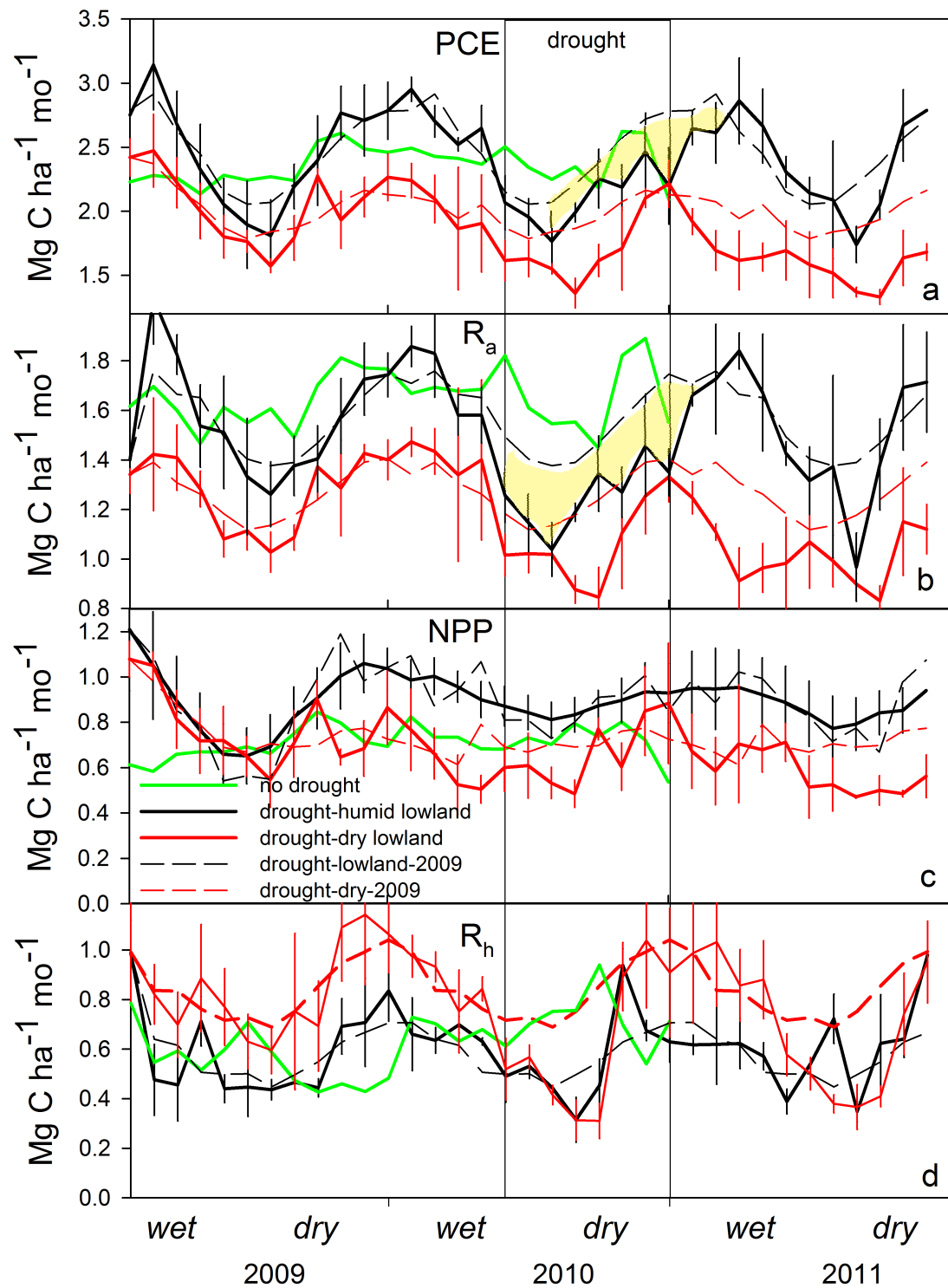
525

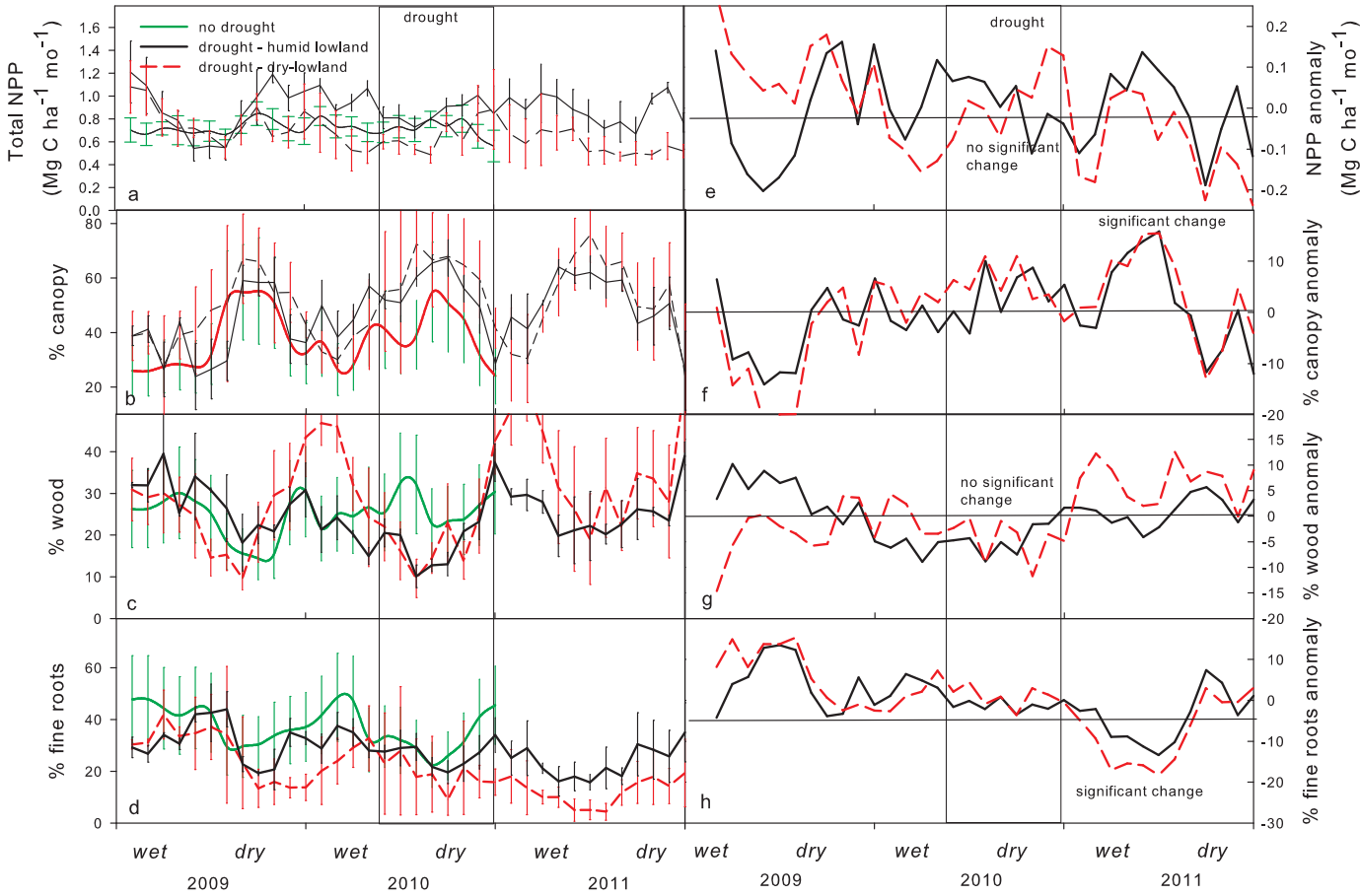
526

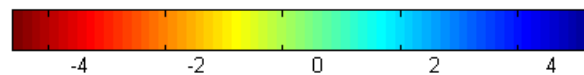
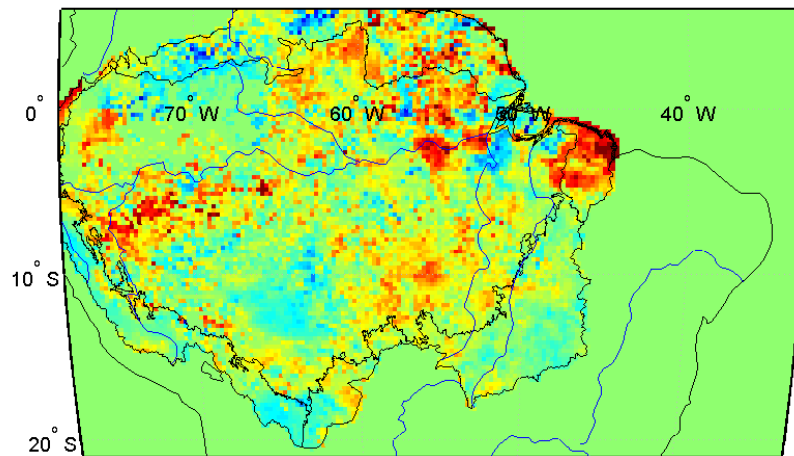
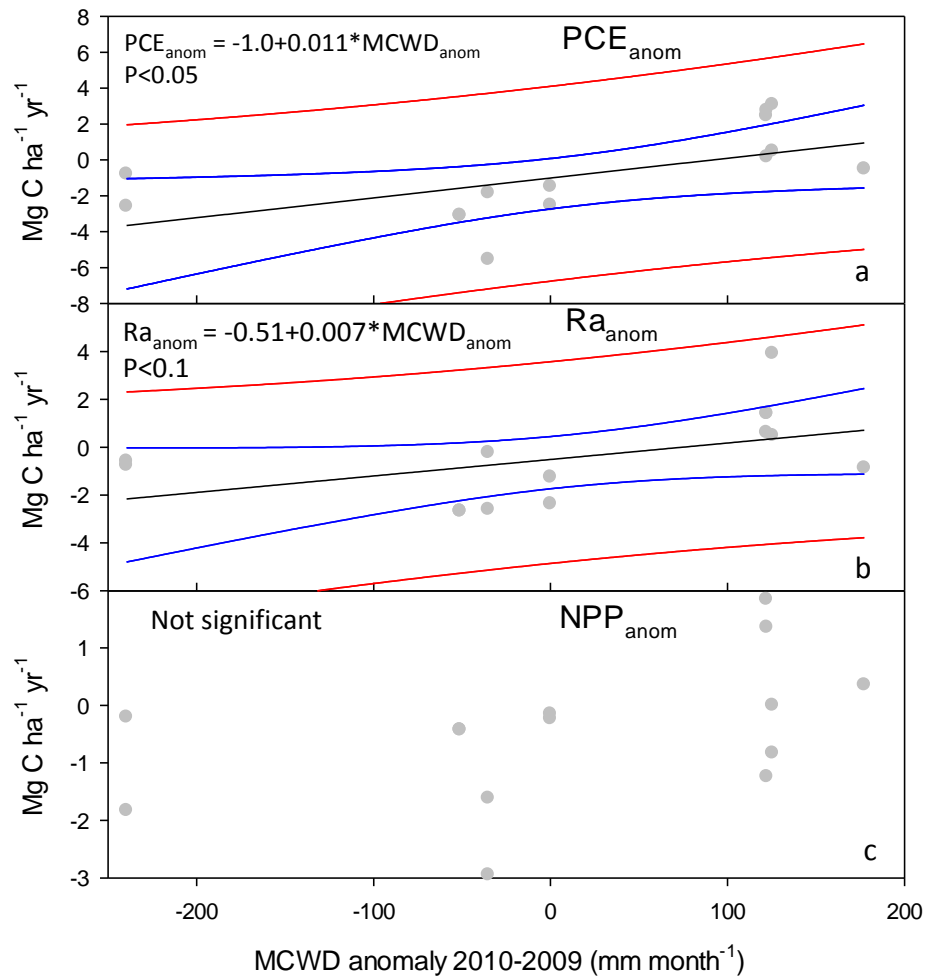
527

529 Additional references

- 530 31 Doughty, C. E. & Goulden, M. L. Seasonal patterns of tropical forest leaf area index and CO₂
531 exchange. *J Geophys Res-Bioge* **113**, -, doi:Artn G00b06 Doi 10.1029/2007jg000590 (2008).
- 532 32 Girardin, C. A. J. *et al.* Productivity and carbon allocation in a tropical montane cloud forest
533 in the Peruvian Andes. *Plant Ecol Divers* **7**, 107-123, doi:Doi 10.1080/17550874.2013.820222
534 (2014).
- 535 33 Huasco, W. H. *et al.* Seasonal production, allocation and cycling of carbon in two mid-
536 elevation tropical montane forest plots in the Peruvian Andes. *Plant Ecol Divers* **7**, 125-142,
537 doi:Doi 10.1080/17550874.2013.819042 (2014).
- 538 34 Quesada, C. A. *et al.* Basin-wide variations in Amazon forest structure and function are
539 mediated by both soils and climate. *Biogeosciences* **9**, 2203-2246, doi:DOI 10.5194/bg-9-
540 2203-2012 (2012).
- 541 35 Lopez-Gonzalez, G., Lewis, S. L., Burkitt, M. & Phillips, O. L. ForestPlots.net: a web application
542 and research tool to manage and analyse tropical forest plot data. *J Veg Sci* **22**, 610-613,
543 doi:DOI 10.1111/j.1654-1103.2011.01312.x (2011).
- 544 36 Feldpausch, T. R. *et al.* Tree height integrated into pantropical forest biomass estimates.
545 *Biogeosciences* **9**, 3381-3403, doi:DOI 10.5194/bg-9-3381-2012 (2012).
- 546 37 Quesada, C. A. *et al.* Soils of Amazonia with particular reference to the RAINFOR sites.
547 *Biogeosciences* **8**, 1415-1440, doi:DOI 10.5194/bg-8-1415-2011 (2011).
- 548 38 Lehmann, J., Kern, D. C., Glaser, B. & Woods, W. I. *Amazonian Dark Earths: Origin,*
549 *Properties, Management.* (Kluwer Academic Publishers, 2003).
- 550 39 Chave, J. *et al.* Tree allometry and improved estimation of carbon stocks and balance in
551 tropical forests. *Oecologia* **145**, 87-99, doi:DOI 10.1007/s00442-005-0100-x (2005).
- 552 40 Doughty, C. E. An In Situ Leaf and Branch Warming Experiment in the Amazon. *Biotropica* **43**,
553 658-665, doi:DOI 10.1111/j.1744-7429.2010.00746.x (2011).
- 554 41 Martin, A. R. & Thomas, S. C. A Reassessment of Carbon Content in Tropical Trees. *Plos One*
555 **6**, doi:ARTN e23533 DOI 10.1371/journal.pone.0023533 (2011).
- 556 42 Metcalfe, D. B. *et al.* Factors controlling spatio-temporal variation in carbon dioxide efflux
557 from surface litter, roots, and soil organic matter at four rain forest sites in the eastern
558 Amazon. *J Geophys Res-Bioge* **112**, doi:Artn G04001 Doi 10.1029/2007jg000443 (2007).
- 559 43 Malhi, Y. *et al.* Exploring the likelihood and mechanism of a climate-change-induced dieback
560 of the Amazon rainforest. *P Natl Acad Sci USA* **106**, 20610-20615, doi:DOI
561 10.1073/pnas.0804619106 (2009).
- 562 44 Chambers, J. Q. *et al.* Respiration from a tropical forest ecosystem: Partitioning of sources
563 and low carbon use efficiency. *Ecol Appl* **14**, S72-S88 (2004).
- 564 45 Malhi, Y. *et al.* Exploring the likelihood and mechanism of a climate-change-induced dieback
565 of the Amazon rainforest. *P Natl Acad Sci USA* **106**, 20610-20615, doi:DOI
566 10.1073/pnas.0804619106 (2009).
- 567 46 da Rocha, H. R. *et al.* Seasonality of water and heat fluxes over a tropical forest in eastern
568 Amazonia. *Ecol Appl* **14**, S22-S32 (2004).
- 569 47 Brando, P. M. *et al.* Abrupt increases in Amazonian tree mortality due to drought-fire
570 interactions. *P Natl Acad Sci USA* **111**, 6347-6352, doi:DOI 10.1073/pnas.1305499111 (2014).







$Mg\ C\ ha^{-1}\ yr^{-1}\ anomaly$

